

Supporting Information for
Fe-N₂/CO complexes that model a possible role for the interstitial C-atom of
FeMoco

Jonathan Rittle, Jonas C. Peters*

*Division of Chemistry and Chemical Engineering,
California Institute of Technology, 1200 E. California Blvd, Pasadena, CA 91125*

[C^{Si}P^{Ph}₃]FeCl (**2**). A red solution of benzyl potassium (50 mg, 385 μ mol) in THF (5 mL) was added in a dropwise fashion to a vigorously stirred solution of [C^{Si}P^{Ph}₃]H (**1**) (300 mg, 382 μ mol) in THF (10 mL) at room temperature. After stirring for 30 min, an aliquot of the orange solution was analyzed by ³¹P NMR spectroscopy to verify consumption of **1** (see below). The solution was cooled to -78 °C and added over 30 min to a pre-chilled solution of FeCl₂(THF)_{1.5} (90 mg, 383 μ mol) in THF (50 mL). The reaction was stirred for an additional hour at -78 °C prior to warming to room temperature. Solvent was removed *in vacuo* and the residue was extracted with CH₂Cl₂ (10 mL). The cloudy yellow solution was filtered via cannula and solvent was removed *in vacuo*. The residue was dissolved in a minimal volume of THF (15 mL) and layered with pentane (30 mL). After standing for 2 days, the solution was decanted and the deposited yellow hexagons were washed with pentane (20 mL) to afford the product (204 mg, 61%). Analytically pure material was prepared by dissolving the hexagons in refluxing benzene, followed by rapid cooling to -35 °C and lyophilization of solvent *in vacuo*. ¹H NMR (CD₂Cl₂, 300 MHz): δ 28.4, 14.5, 11.3, 0.41. UV-Vis (THF, nm {cm⁻¹ M⁻¹}): 335 {2700}. μ_{eff} (CD₂Cl₂, Evans method, 20 °C): 4.8 μ_{B} . Anal: calc. for C₄₆H₅₄ClFeP₃Si₃: C 63.11, H 6.22; found: C 63.39, H 6.21.

[C^{Si}P^{Ph}₃]Fe (**3**). Sodium (10.5 mg, 465 μ mol) was combined with mercury (2.10 g) in a scintillation vial. A solution of **2** (200 mg, 229 μ mol) in THF (5 mL) was added with a stir bar. The mixture was vigorously stirred overnight as a dark red color developed. The solution was

filtered through celite and solvent evaporated *in vacuo*. The residue was dissolved in minimal pentane (20 mL), filtered through celite and evaporated to dryness *in vacuo*. The residue was taken up in benzene (5 mL), frozen and lyophilized yielding analytically pure **3** (169 mg, 88%) as a brick red powder. XRD-quality crystals were grown by slow evaporation of a concentrated solution of **3** in benzene. ^1H NMR (C_6D_6 , 300 MHz): δ 11.45, 7.47, 4.20, 4.08. UV-Vis (THF, nm $\{\text{cm}^{-1} \text{M}^{-1}\}$): 306 {10300}, 350 {6930}, 465 {3250}, 820 {865}. μ_{eff} (C_6D_6 , Evans method, 20 °C): 3.8 μ_{B} . Anal: calc. for $\text{C}_{46}\text{H}_{54}\text{FeP}_3\text{Si}_3$: C 65.78, H 6.48; found: C 65.11, H 6.30.

{K(benzo-15-crown-5)}₂}{[C^{SiPh}P^{Ph}]₃FeN₂} (**4**). A solution of **3** (36.3 mg, 43.2 μmol) in THF (5 mL) was charged with a stir bar and cooled to -78 °C. A solution of KC_8 (7 mg, 51.9 μmol) in THF (2 mL) was added dropwise over 5 minutes, causing a dramatic color change to inky purple. A solution of benzo-15-crown-5 (24.3 mg, 90.7 μmol) in THF (2 mL) was added and the mixture was brought to rt and stirred for 1 hr. The mixture was filtered through celite and evaporated to dryness *in vacuo*. The residue was washed with pentane (5 mL) and Et_2O (3 x 5 mL) affording **4** as a dark purple powder (39.3 mg, 63%). XRD-quality crystals were grown by diffusion of pentane vapors into a concentrated THF solution of **4**. ^1H NMR (d_8 -THF, 400 MHz, 20 °C): δ 7.10 (m, 18 H), 6.77 (m, 20H), 4.04 (s, 6H), 3.89 – 3.41 (m, 32H), 1.70 (s, 6H), 0.10 (s, 9H), -0.13 (s, 9H). ^{31}P NMR (d_8 -THF, 121 MHz): δ 43.0. UV-Vis (THF, nm $\{\text{cm}^{-1} \text{M}^{-1}\}$): 422 {7930}, 535 {10160}. IR (KBr): $\nu_{\text{NN}} = 1927 \text{ cm}^{-1}$. Satisfactory combustion analysis could not be obtained due to the lability of the N_2 ligand under prolonged exposure to vacuum.

[κ_3 - C^{SiPh}P^{Ph}]₃ Fe(NNTIPS) (**5**) To a vigorously stirred suspension of **4** (100 mg, 69 μmol) in benzene (5 mL) was added triisopropylsilyl trifluoromethanesulfonate (56.6 mg, 68 μmol) diluted in benzene (2 mL) in one portion. The suspension was allowed to stir for 2 hr at rt causing the development of a dark brown solution. Pentane (10 mL) was added and the resulting

mixture was stirred for 15 min at rt. The solution was subsequently filtered and evaporated to dryness *in vacuo*. The dark residue was reconstituted in pentane spiked with HMDSO and allowed to slowly evaporate overnight. Large dark rhomboids (suitable for XRD) formed and were washed with HMDSO (3 x 2 mL) and pentane (2 mL) furnishing **5** (41.7 mg, 59%) as a dark mahogany solid. ^1H NMR (d_8 -Toluene, 300 MHz, 20 °C): δ 7.72, 5.35, 4.18, -1.76. UV-Vis (2-MeTHF, nm { $\text{cm}^{-1} \text{M}^{-1}$ }): 505 {940}, 785 {240}. μ_{eff} (C_6D_6 , Evans method, 20 °C): 2.75(2) μ_{B} . IR (KBr): $\nu_{\text{NN}} = 1719 \text{ cm}^{-1}$. Multiple attempts at obtaining combustion analysis on crystalline material consistently indicated low nitrogen and high carbon content. Representative C, H, N Anal: calc. for $\text{C}_{55}\text{H}_{75}\text{FeN}_2\text{P}_3\text{Si}_4$: C 64.43, H 7.37, N 2.73; found: C 61.54, H 7.44, N 1.25.

[C^{SiPh}₃]FeCO (6). A solution of **3** (51.3 mg, 61.1 μmol) in Et_2O (5 mL) was charged into a Schlenk tube with a magnetic stir bar. A mild static vacuum was applied to the vessel for 10 minutes. An atmosphere of CO was introduced and the solution was stirred for 30 minutes causing a slight color change. Solvent was evaporated *in vacuo* and the residue was washed with pentane (5 mL). The orange red powder was dissolved in benzene (5 mL), frozen and lyophilized yielding analytically-pure **6** (47.7 mg, 90%). XRD-quality crystals were grown by diffusion of pentane vapors into a concentrated benzene solution of **6**. ^1H NMR (C_6D_6 , 300 MHz, 20 °C): δ 14.70, 9.17, 4.28, 3.43, 1.78. UV-Vis (THF, nm { $\text{cm}^{-1} \text{M}^{-1}$ }): 389 {6850}, 485 {3210}, 911 {350}. μ_{eff} (C_6D_6 , Evans method, 20 °C): 1.5 μ_{B} . IR (KBr): $\nu_{\text{CO}} = 1850 \text{ cm}^{-1}$. Anal: calc. for $\text{C}_{47}\text{H}_{54}\text{FeOP}_3\text{Si}_3$: C 64.96, H 6.38; found: C 64.94, H 6.36.

{K(benzo-15-crown-5)}₂{[C^{SiPh}₃]FeCO} (7). A solution of **6** (34 mg, 50 μmol) in THF (5 mL) was charged with a stir bar and cooled to -78 °C. A solution of KC_8 (14.7 mg, 109 μmol) in THF (2 mL) was added in a dropwise fashion over 5 minutes, initiating a color change to purple. A solution of benzo-15-crown-5 (29 mg, 108 μmol) in THF (2 mL) was added and the mixture was

brought to rt and stirred for 1 hr. The mixture was filtered through celite and evaporated to dryness *in vacuo*. The residue was washed with pentane (5 mL) and Et₂O (3 x 5 mL) affording **6** as a dark burgundy powder (49 mg, 87 %). XRD-quality crystals were grown by diffusion of pentane vapors into a concentrated THF solution of **6**. ¹H NMR (d₈-THF, 400 MHz, 20 °C): δ 7.16 (s, 12H), 6.87 (m, 8H), 6.72 (br m, 18H) 3.81 (m, 8H), 3.66 (m, 16H), 3.60 (m, 8H), 1.88 (s, 6H) 0.06 (s, 18H). ³¹P NMR (d₈-THF, 121 MHz): δ 51.3. UV-Vis (THF, nm {cm⁻¹ M⁻¹}): 403 {5630}, 502 {8230}. IR (KBr): ν_{CO} = 1782 cm⁻¹.

[[C^{SiP^{Ph}}₃]FeCO]{B(3,5-(CF₃)₂-C₆H₃)₄} (8**).** To a suspension of {Cp₂Fe}{B(3,5-(CF₃)₂-C₆H₃)₄} (35 mg, 33.4 μmol) in benzene (2 mL) was added a solution of **6** (30 mg, 34.5 μmol) in benzene (2 mL) with rapid stirring. After 5 minutes, pentane (15 mL) was added dropwise, causing the precipitation of a fine light orange solid. The solid was collected on glass filter paper, washed with benzene (2 mL) and pentane (2 mL) and dried with a stream of N₂ furnishing spectroscopically pure **8** (34 mg, 57%). ¹H NMR (CD₂Cl₂, 300 MHz, 20 °C): δ 58.01, 17.93, 12.33, 7.75, 7.58, 3.25, 0.47, 0.59. UV-Vis (Et₂O, nm {cm⁻¹ M⁻¹}): 319 {5800}, 407 {3400}, 436 {3100}, ~1100 {350}. μ_{eff} (CD₂Cl₂, Evans method, 20 °C): 2.79 μ_B. IR (KBr): ν_{CO} = 1937 cm⁻¹. Application of dynamic vacuum to the resulting powder results in substantial decomposition as evidenced by ¹H NMR and IR spectroscopy. Hence, combustion analysis was not attempted.

Toepler Pump Experiment. A solution of **4** (58.1 mg, 40 μmol) dissolved in THF (5 mL) was added to a Schlenk flask fitted with a solid addition arm containing ferrocenium trifluoromethanesulfonate (39 mg, 200 μmol). The apparatus was evacuated and subjected to four freeze-pump-thaw cycles to eliminate any atmospheric N₂. While vigorously stirring the solution, the ferrocenium salt was added in one portion, causing an immediate effervescence and

solution color change to orange. Toepler analysis of the resulting atmosphere suggested the formation of dinitrogen (36 μmol , 90%).

Spectra

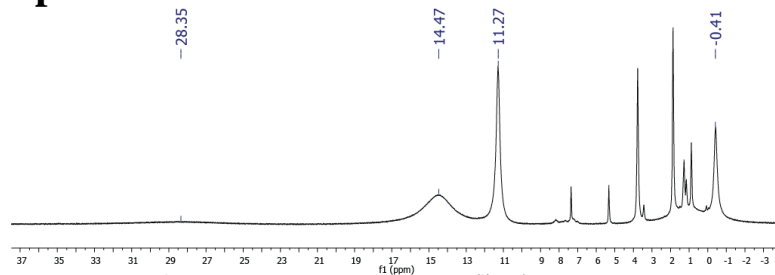


Figure S1. ^1H NMR spectrum of $[\text{C}^{\text{SiP}^{\text{Ph}}_3}\text{FeCl}]$ (**2**) (CD_2Cl_2 , r.t.).

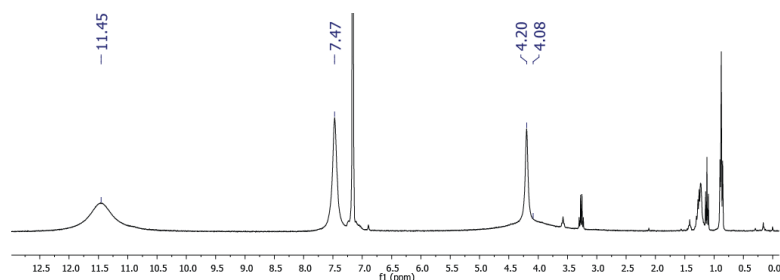


Figure S2. ^1H NMR spectrum of $[\text{C}^{\text{SiP}^{\text{Ph}}_3}\text{Fe}]$ (**3**) (C_6D_6 , r.t.).

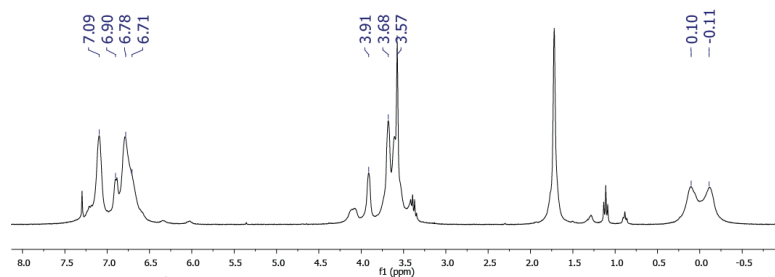


Figure S3. ^1H NMR spectrum of $\{\text{K}(\text{Benzo-15-crown-5})_2\}\{[\text{C}^{\text{SiP}^{\text{Ph}}_3}\text{FeN}_2]\}$ (**4**) ($d_8\text{-THF}$, r.t.).

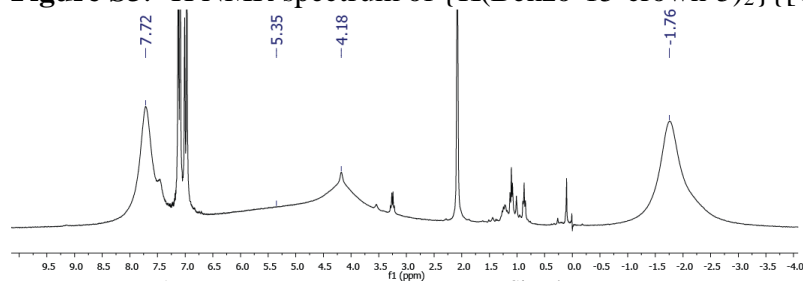


Figure S4. ^1H NMR spectrum of $[\kappa^3\text{-C}^{\text{SiP}^{\text{Ph}}_3}\text{Fe}(\text{NNTIPS})]$ (**5**) (C_7D_8 , r.t.).

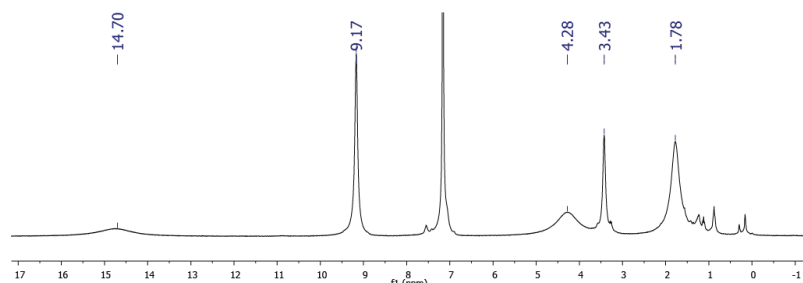


Figure S5. ^1H NMR spectrum of $[\text{C}^{\text{SiP}^{\text{Ph}}_3}\text{FeCO}]$ (**6**) (C_6D_6 , r.t.).

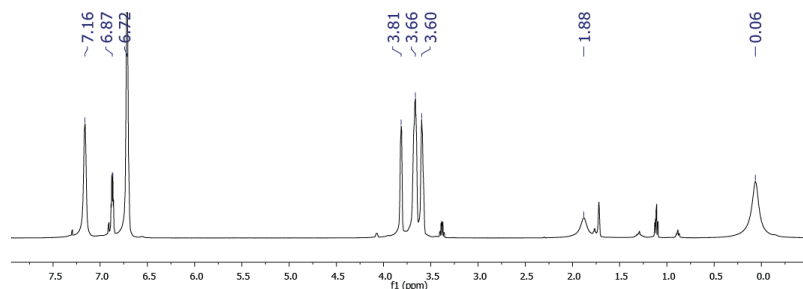


Figure S6. ^1H NMR spectrum of $\{\text{K}(\text{benzo-15-crown-5})_2\}\{[\text{C}^{\text{SiP}^{\text{Ph}}_3}\text{FeCO}]\}$ (**7**) ($\text{d}_8\text{-THF}$, r.t.).

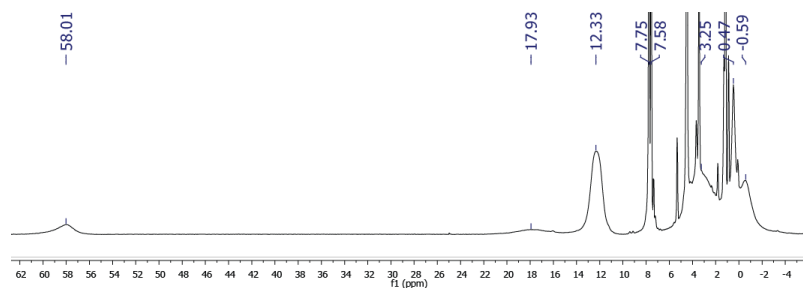


Figure S7. ^1H NMR spectrum of $\{\text{C}^{\text{SiP}^{\text{Ph}}_3}\text{FeCO}\}\{\text{B}(3,5\text{-(CF}_3)_2\text{-C}_6\text{H}_3)_4\}$ (**8**) (CD_2Cl_2 , r.t.).

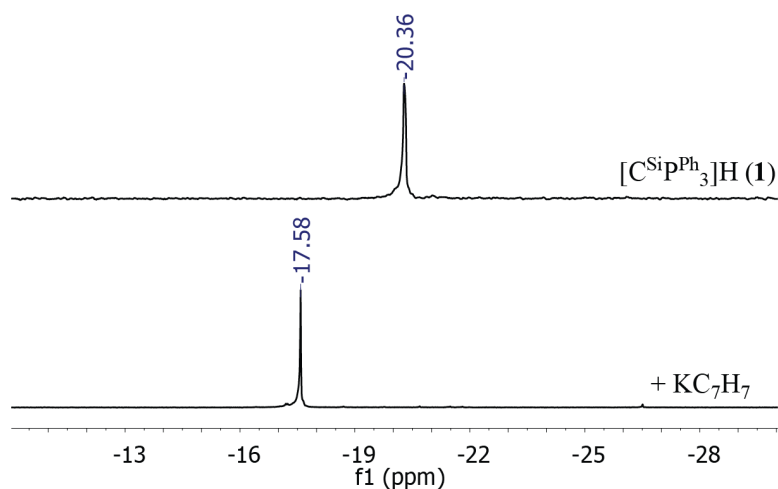


Figure S8. ^{31}P NMR spectra of (top) $[\text{C}^{\text{SiP}^{\text{Ph}}_3}\text{H}]$ (**1**) before and (bottom) after addition of benzyl potassium (THF, r.t.).

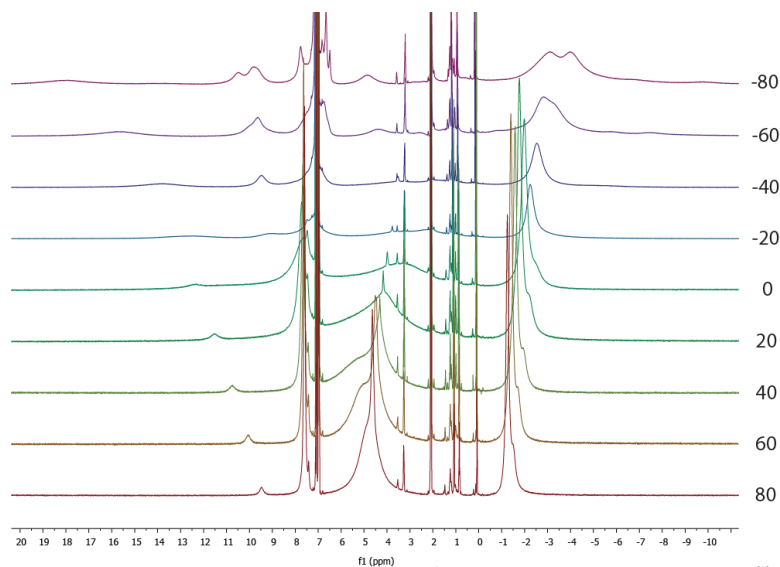


Figure S9 Variable temperature ^1H NMR spectra of $[\kappa_3\text{-C}^{\text{SiPh}_3}]\text{Fe}(\text{NNTIPS})$ in d_8 -toluene. Temperatures listed in $^\circ\text{C}$.

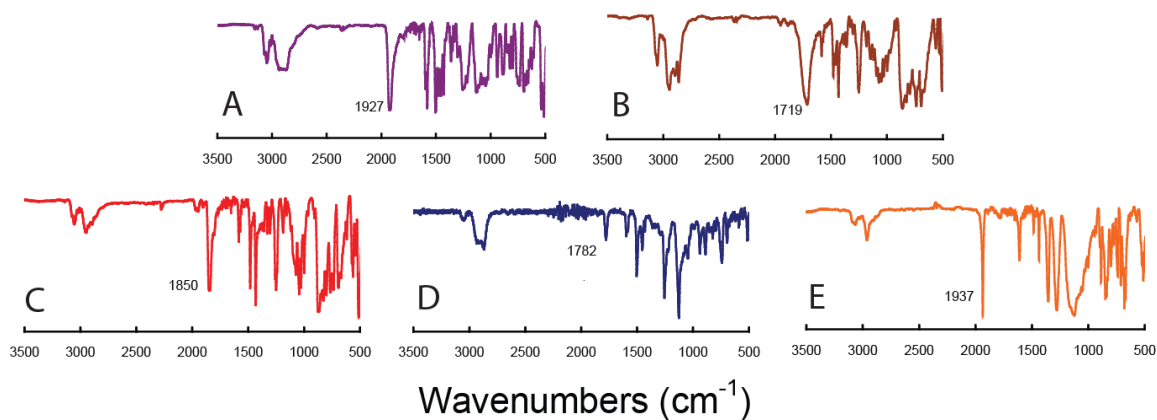


Figure S10. IR spectra of **4** (A), **5** (B), **6** (C), **7** (D), and **8** (E) in KBr pellets.

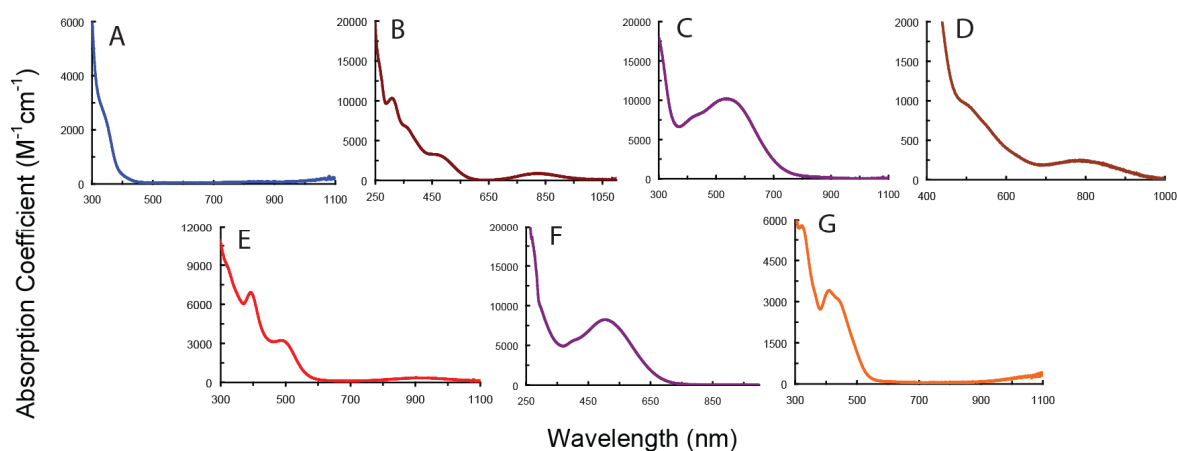


Figure S11. UV-Visible spectra of **2** (A) in THF, **3** (B) in THF, **4** (C) in THF, **5** (D) in 2-MeTHF, **6** (E) in THF, **7** (F) in THF, and **8** (G) in Et_2O .

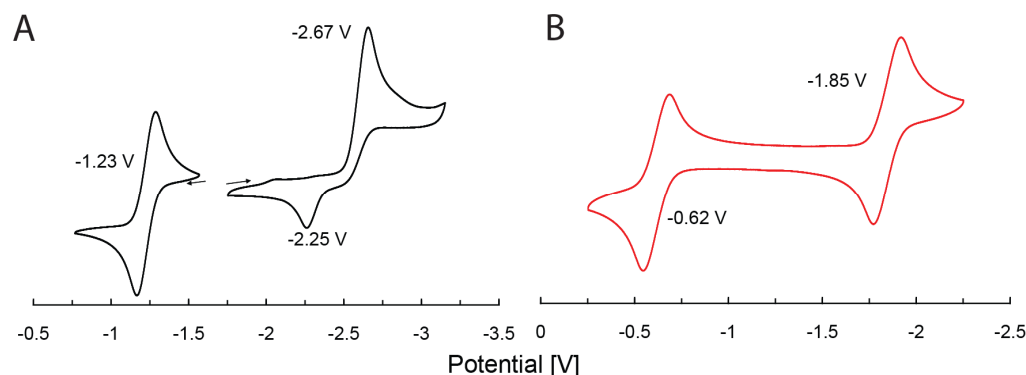


Figure S12. Cyclic voltammograms of (A) $[\text{C}^{\text{SiP}^{\text{Ph}}_3}\text{Fe}]$ (**3**, 1 mM) and (B) $[\text{C}^{\text{SiP}^{\text{Ph}}_3}\text{FeCO}]$ (**6**, 1 mM) recorded with a scan rate of 50 mV/s in 0.3M tetra-*n*-butylammonium hexafluorophosphate in THF.

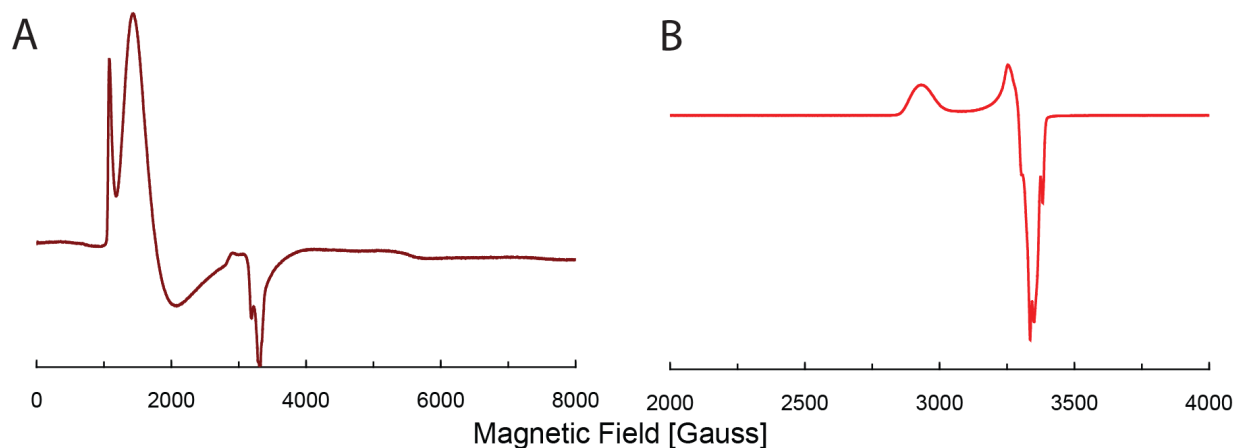


Figure S13. X-band EPR spectra of (A) $[\text{C}^{\text{SiP}^{\text{Ph}}_3}\text{Fe}]$ (**3**) and (B) $[\text{C}^{\text{SiP}^{\text{Ph}}_3}\text{FeCO}]$ (**6**) in 2-MeTHF at 10K.

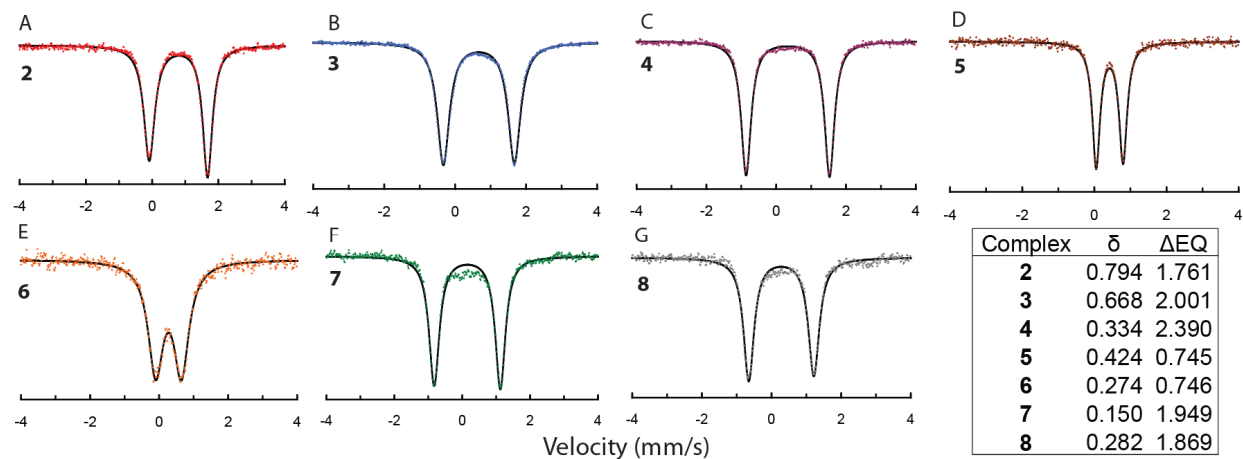


Figure S14. Zero-field Mössbauer spectra of reported compounds (A – G, **2** – **8**, respectively) recorded at 80K in boron nitride pellets. The solid lines represent fits using Lorentzian lineshapes with the resulting parameters tabulated in the inset.

X-Ray Diffraction Data

Special Refinement Details for Compound 4

The structure is disordered in one of the ethylene linkers of the cation. The carbon atoms are split in two positions but the occupancy of the minor position is <30% and could not be modeled effectively. This results in an unusually large U_{eq} for atoms C70A and C68A that could not be remedied with ISOR restraints. Work is in progress to obtain a higher quality crystal structure of 4.

Special Refinement Details for Compound 7

The structure is disordered in one of the ethylene linkers of the cation. The carbon atoms are split in two positions of equal occupancy but C305 appears to be further split into two subpositions and could not be modeled effectively. This results in an unusually prolate ellipsoid for atom C305 that could not be remedied by using ISOR restraints or splitting the position.

Table S1. Crystallographic Data for Compounds **2** - **8**

compound	2	3	4	5	6
chem formula	C ₅₈ H ₇₂ ClFeP ₃ Si ₃	C ₄₉ H ₅₇ FeP ₃ Si ₃	C ₇₄ H ₉₆ FeKN ₂ O ₁₀ P ₃ Si ₃	C ₅₅ H ₇₅ FeN ₂ P ₃ Si ₄	C ₄₇ H ₅₄ FeOP ₃ Si ₃
fw	1037.64	878.98	1445.66	1025.29	867.93
cryst syst	Hexagonal	Triclinic	Monoclinic	Triclinic	Triclinic
space group	P - 3	P - 1	P2 ₁ /n	P - 1	P - 1
a [Å]	13.7360(3)	13.5943(5)	17.1406(18)	11.8919(7)	12.4071(5)
b [Å]	13.7360(3)	13.6693(7)	24.806(3)	12.0676(7)	18.5776(8)
c [Å]	14.9437(4)	15.1312(6)	17.5292(19)	19.8638(12)	30.0665(13)
α [°]	90	91.235(3)	90	84.883(4)	106.994(3)
β [°]	90	106.027(2)	93.561(5)	88.188(4)	93.950(2)
γ [°]	120	119.307(2)	90	84.210(4)	94.012(2)
V [Å ³]	2441.79(10)	2315.02(17)	7438.8(14)	2824.0(3)	6582.3(5)
Z	2	2	4	2	6
D _{calcd} [g cm ⁻³]	1.411	1.261	1.291	1.206	1.314
F(000)	1100	928	3064	1092	2742
μ [mm ⁻¹]	0.577	0.54	0.429	0.473	0.57
temp [K]	100	100	100	200	100
wavelength [Å]	0.71073	0.71073	0.71073	0.71073	0.71073
measurd reflns	89768	45273	161024	303132	273978
unique reflns	10664	11297	18479	28008	54166
data/restraints/param	10664/6/181	11297/0/505	18479/12/847	28008/x/598	54166/0/1505
R(F) (I>2σ(I))	0.0507	0.0399	0.095	0.0534	0.0623
wR(F ²) (all)	0.1424	0.0964	0.286	0.1563	0.1604
GOF	1.037	1.038	1.058	1.028	1.009

Table S1 cont.

	7	8
chem formula	C ₇₈ H ₉₇ FeKO ₁₁ P ₃ Si ₃	C ₈₂ H ₈₀ BF ₂₄ FeO ₂ P ₃ Si ₃
fw	1482.69	1797.30
cryst syst	Monoclinic	Monoclinic
space group	P2 ₁ /c	P2 ₁ /c
a [Å]	24.1138(16)	18.4849(8)
b [Å]	24.5835(17)	21.1656(9)
c [Å]	25.0501(17)	21.2880(8)
α [°]	90	90
β [°]	90.013(4)	101.584(2)
γ [°]	90	90
V [Å ³]	14849.7(17)	8159.2(6)
Z	8	4
D _{calcd} [g cm ⁻³]	1.326	1.463
F(000)	6280	3688
μ [mm ⁻¹]	0.432	0.390
temp [K]	100	100
wavelength [Å]	0.71073	0.71073
measurd reflns	353982	300721
unique reflns	46528	17791
data/restraints/param	46528/0/1775	17791/0/1052
R(F) (I>2σ(I))	0.0615	0.0428
wR(F ²) (all)	0.1781	0.1150
GOF	1.047	1.019

Table S2. Structural parameters of **6** illustrating the deviance from threefold symmetry.

a,b	Molecule 1	Molecule 2	Molecule 3
Fe-C _{alkyl}	2.227(2)	2.239(4)	2.244(3)
Fe-C _{CO}	1.729(3)	1.736(3)	1.737(3)
Fe-P1	2.3260(7)	2.3263(7)	2.3273(8)
Fe-P2	2.3011(7)	2.2964(7)	2.2919(8)
Fe-P3	2.2814(7)	2.2807(7)	2.2773(8)
P1-Fe-P2	111.43(3)	115.20(3)	134.17(3)
P1-Fe-P3	133.70(3)	136.45(3)	115.16(3)
P2-Fe-P3	114.86(3)	108.34(3)	110.67(3)
C _{alkyl} -Fe-C _{CO}	178.1(1)	174.9(1)	174.4(1)
Tau	0.74	0.64	0.67

^a Distances listed in Å. ^b Angles listed in degrees.

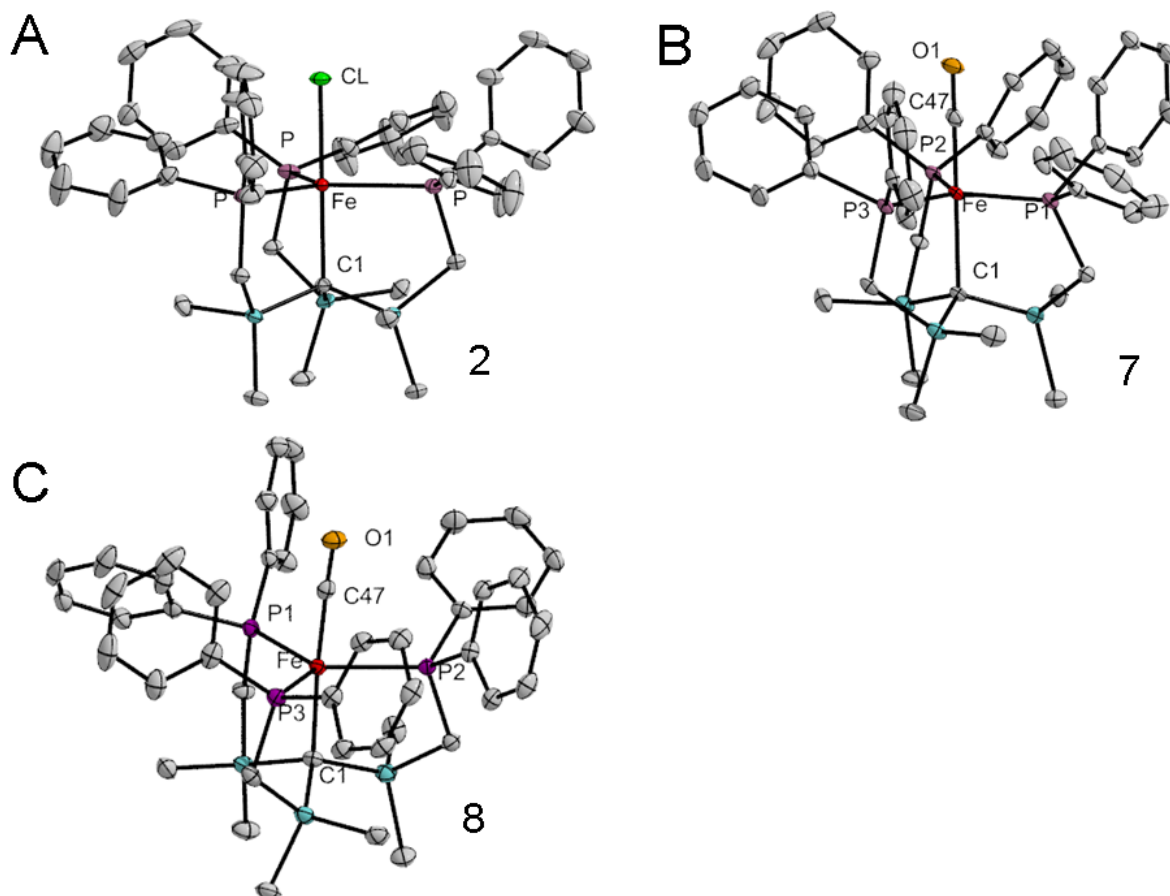


Figure S15. Solid-state structures of (A) $[\text{C}^{\text{SiP}^{\text{Ph}}_3}\text{FeCl}]$ (**2**), (B) $\{\text{K}(\text{benzo-15-crown-5})_2\}\{[\text{C}^{\text{SiP}^{\text{Ph}}_3}\text{FeCO}]\}$ (**7**), and (C) $\{[\text{C}^{\text{SiP}^{\text{Ph}}_3}\text{FeCO}]\}\{\text{B}(3,5\text{-(CF}_3)_2\text{-C}_6\text{H}_3)_4\}$ (**8**). Thermal ellipsoids set at 50% probability. For clarity, one molecule of **7**, hydrogen atoms, the $\text{B}(3,5\text{-(CF}_3)_2\text{-C}_6\text{H}_3)_4$ anion of **8** and co-crystallized solvent have been omitted.

Optimized Coordinates of 12 and 13

12

```
C 0.20655756 -1.05675356 -1.42064351
C 0.22393762 -0.70054683 1.62392177
C 0.19577328 1.76016386 -0.20648787
C -1.76191239 -0.01067465 0.01071375
Fe 0.01511268 0.00033537 -0.00017796
O 0.38397278 -1.74795068 -2.34916867
O 0.41276697 -1.15843359 2.68507774
O 0.36620062 2.91082358 -0.34189965
O -2.93040264 -0.01775967 0.01773879
C 2.15862379 0.01517014 -0.01410136
H 2.52698900 0.43029282 -0.95756284
H 2.53741895 0.62654807 0.81105074
H 2.54448145 -1.00315128 0.09673667
```

13

```
C -0.89424425 -0.67335468 1.66991020
C -0.89493577 1.78257799 -0.25070893
C -0.89414632 -1.11144496 -1.41576152
```

```
C -2.66921420 0.00023663 -0.00098335
Fe -0.90123617 -0.00012013 0.00027934
O -0.98665469 -1.10915569 2.74562602
O -0.98836643 2.93203444 -0.41116454
O -0.98589019 -1.82704543 -2.32962878
O -3.83333306 0.00054192 -0.00237336
C 1.34939799 -0.00016184 -0.00073097
H 1.45040178 -0.06187850 -2.80948452
H 1.59209580 2.11983460 -1.81816476
H 3.45653111 0.64478647 -1.74550828
H 1.47085148 2.47060078 1.33179561
H 1.57570266 0.53124537 2.74321270
H 3.45976166 1.17135112 1.44038261
H 1.47304520 -2.38923309 1.47286088
H 1.57552926 -2.64222573 -0.91209527
H 3.46073255 -1.83309035 0.29136077
Si 1.95763194 0.68691991 -1.62506596
Si 1.96062568 -1.74904733 0.21832788
Si 1.95962089 1.06452826 1.4044
```

Discussion of the use of the τ_5 and τ_4 parameters

Compounds **2**, **4**, and **6 – 8** are five coordinate Fe complexes in a pseudo-trigonal bipyramidal geometry. The geometric distortion away from a perfect trigonal bipyramid occurs predominately within the plane of the phosphines, such that one P-Fe-P angle becomes larger, and thus the geometry begins approaching that of a square pyramid. As these compounds are all somewhere on the continuum between these two geometric extremes, we utilize a parameter, τ_5 , (6) to quantitatively describe their geometries. A perfect trigonal bipyramid displays a τ_5 value of 1.00 and a perfect square pyramid displays a value of 0.00.

Compound **3** is a four coordinate complex in a geometry intermediate between tetrahedral and trigonal pyramidal. Similar to the case above, we desire to quantify the geometry between these two extremes. Hollands τ_4 parameter (ref 30 in main text) is ideal, and allows a comparison to the belt Fe atoms of FeMoco. A τ_4 value of 1.00 corresponds to a perfect trigonal pyramid and a value of 0.00 corresponds to a perfect tetrahedron.

References

1. Evans DF (1959) The determination of the paramagnetic susceptibility in solution by nuclear magnetic resonance. *J Chem Soc* 2003-2005.
2. Sur SK (1989) Measurement of magnetic susceptibility and magnetic moment of paramagnetic molecules in solution by high-field Fourier transform NMR spectroscopy. *J Magn Reson* 82:169-173.
3. Sheldrick GM (2008) A short history of SHELX. *Acta Cryst A* 64:112-122.
4. Gaussian 03, Revision C.02, Frisch, M. J.; Trucks, G. W.; Schlegel, H. B.; Scuseria, G. E.; Robb, M. A.; Cheeseman, J. R.; Montgomery, Jr., J. A.; Vreven, T.; Kudin, K. N.; Burant, J. C.; Millam, J. M.; Iyengar, S. S.; Tomasi, J.; Barone, V.; Mennucci, B.; Cossi, M.; Scalmani, G.; Rega, N.; Petersson, G. A.; Nakatsuji, H.; Hada, M.; Ehara, M.; Toyota, K.; Fukuda, R.; Hasegawa, J.; Ishida, M.; Nakajima, T.; Honda, Y.; Kitao, O.; Nakai, H.; Klene, M.; Li, X.; Knox, J. E.; Hratchian, H. P.; Cross, J. B.; Bakken, V.; Adamo, C.; Jaramillo, J.; Gomperts, R.; Stratmann, R. E.; Yazyev, O.; Austin, A. J.; Cammi, R.; Pomelli, C.; Ochterski, J. W.; Ayala, P. Y.; Morokuma, K.; Voth, G. A.; Salvador, P.; Dannenberg, J. J.; Zakrzewski, V. G.; Dapprich, S.; Daniels, A. D.; Strain, M. C.; Farkas, O.; Malick, D. K.; Rabuck, A. D.; Raghavachari, K.; Foresman, J. B.; Ortiz, J. V.; Cui, Q.; Baboul, A. G.; Clifford, S.; Cioslowski, J.; Stefanov, B. B.; Liu, G.; Liashenko, A.; Piskorz, P.; Komaromi, I.; Martin, R. L.; Fox, D. J.; Keith, T.; Al-Laham, M. A.; Peng, C. Y.; Nanayakkara, A.; Challacombe, M.; Gill, P. M. W.; Johnson, B.; Chen, W.; Wong, M. W.; Gonzalez, C.; and Pople, J. A.; Gaussian, Inc., Wallingford CT, 2004.
5. Becke AD (1993) Density-functional thermochemistry. III. The role of exact exchange. *J Chem Phys* 98:5648-5652.
6. Addison AW, Rao TN, Reedijk J, van Rijn J, Verschoor GC (1984) Synthesis, structure, and spectroscopic properties of copper(II) compounds containing nitrogen-sulphur donor ligands; the crystal and molecular structure of aqua[1,7-bis(N-methylbenzimidazol-2'-yl)-2,6-dithiaheptane]copper(II) perchlorate. *J Chem Soc Dalton Trans* 1349-1356.